

# Application of Temporally Constrained Compressed Sensing for High Spatial and Temporal Resolution Intracranial CE MRA

J. V. Velikina<sup>1</sup>, K. M. Johnson<sup>1</sup>, S. R. Kecskemeti<sup>1</sup>, P. A. Turski<sup>2</sup>, and A. A. Samsonov<sup>1,2</sup>

<sup>1</sup>Medical Physics, University of Wisconsin - Madison, Madison, WI, United States, <sup>2</sup>Radiology, University of Wisconsin - Madison

**Introduction.** Time-resolved contrast-enhanced MR angiography has shown utility in demonstrating intracranial arterial and venous pathology [1]. However, the need for high spatial resolution and signal-to-noise ratio (SNR) often limit the temporal resolution to the levels inadequate for depiction of vessel filling dynamics in intracranial MRA. In the recent years, a number of constrained reconstruction methods that exploit inherent redundancies in the temporal image series [2-5] have been proposed with the aim to increase achievable acceleration factors by improving SNR and artifact level of images obtained from incomplete k-space data. In particular, temporally constrained compressed sensing (TC CS) was shown to allow acceleration factors up to 13 in 2D phase contrast imaging [5]. The goal of this work is a systematic study of the performance of TC CS reconstruction for applications in time-resolved contrast-enhanced neuro-angiography.

**Theory and Methods.** TC CS is applied by solving the following optimization problem:  $f = \arg \min_f (\|Ef - b\|_2^2 + \lambda \|\Delta_t^2 f\|_{l_1/l_2})$ , where  $f$  is the underlying signal vector comprising all time frames,  $E$  is encoding matrix for all time frames, consisting of both Fourier terms and coil sensitivities,  $b$  is the measured k-space data,  $\lambda$  is regularization parameter providing balance between the data fidelity and penalty terms. We chose to penalize the discrete 2<sup>nd</sup> derivative  $\Delta_t^2$  in the time dimension based on the fact that for each pixel temporal progression should be either smoothly varying with the contrast uptake (2<sup>nd</sup> derivative is small) or constant in the stationary tissue (2<sup>nd</sup> derivative is zero). Therefore,  $\Delta_t^2$  operator should sparsify the image volume in  $x$ - $t$  space. The hybrid  $l_1/l_2$  norm [6] was chosen for its ability both to promote sparsity and to optimize noise properties.

As a part of an ongoing large study, the algorithm was applied to image reconstruction of highly undersampled data from human subjects, including three patients with intracranial aneurysms. Following informed consent according to the IRB at our institution, all human subjects were scanned on a 3.0

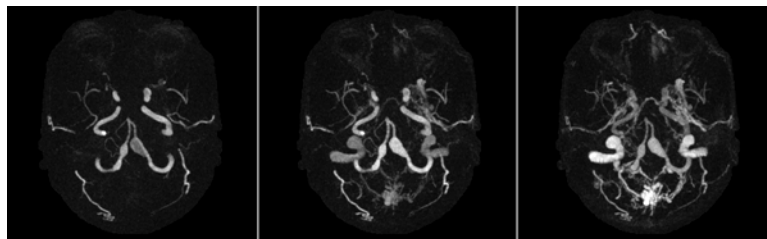


**Figure 1.** TC CS reconstruction of 3 representative time frames (3.6 s intervals).

T clinical scanner (Discovery<sup>TM</sup> MR750, GE Healthcare, Waukesha, WI) using a hybrid radial (in-plane)/Cartesian (through-plane) acquisition during a contrast injection. The scan parameters were TE/TR=1.5/4 ms, FA=25°, BW=125 kHz, 20 slices, voxel size 0.86x0.86x2 mm<sup>3</sup>. All exams but one used an 8-channel head coil, while one volunteer scan was performed using a 32-channel coil to test its utility in the study. The data were then reconstructed using both iterative SENSE [7] and TC CS as described above from 15 radial projections per slice per 1.2 s time frame (acceleration factor R=27).

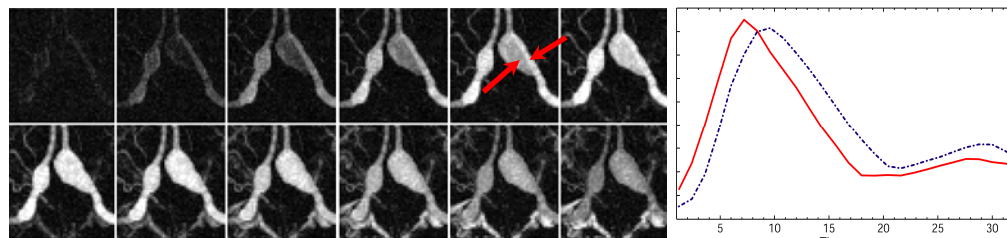


**Figure 2.** (a) Filling of the aneurysms; (b) Temporal waveforms in one of the aneurysms (dashed line) and its feeding artery (solid line) measure at the locations marked by arrows.

**Results.** Images in Fig. 1 depict three frames with different filling stages of an aneurysm patient exam reconstructed with TC CS, while images in Fig. 2a zoom in on the aneurysms demonstrating temporal progression of contrast uptake and wash out. Plots in Fig. 2b correspond to temporal waveforms in one of the aneurysms and its feeding artery.

Note that our temporal resolution is sufficient to demonstrate that filling of the aneurysm is significantly delayed compared to the artery. Images in Fig. 3a-b compare a single frame reconstruction results in a healthy volunteer using iterative SENSE and TC CS from data acquired with a 32-channel coil. Note the high spatial resolution and g-factor suppression in the TC CS image. Excellent arterial/venous separation even in small vessels is confirmed by contrast uptake plots in Fig. 3c. In the SENSE reconstruction (dashed lines), the chosen small vein is indiscernible behind the noise, thus, its waveform does not provide temporal information. However, arterial waveform from the SENSE reconstruction confirms correct representation of temporal behavior by TC CS (solid lines), which provides a clear depiction of even small vessels. Such comparison was not possible in the 8-channel coil acquisition due to inferior image quality of SENSE reconstruction (results not shown here).

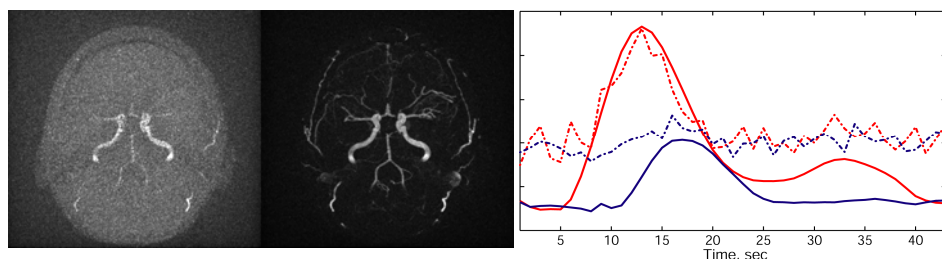


**Figure 3.** Single arterial time frame reconstructed with (a) SENSE; (b) temporally constrained CS; (c) comparison of temporal waveforms in a small artery (red) and neighboring vein (blue).

**Discussion and Conclusions.** TC CS method was shown to be an attractive reconstruction approach that enables 3D time-resolved contrast-enhanced intracranial angiography at high spatial (0.86 x 0.86 x 2 mm<sup>3</sup>) and temporal (1.2 s) resolution for improved diagnostic quality. The obtained resolution was shown to be sufficient to resolve different filling patterns of healthy and pathological vasculature. As part of an ongoing clinical study, we will apply TC CS to exams of patients with arterial stenoses and arterio-venous malformations, where temporal information is important for diagnosis and selection of treatment options. The use of a 32-channel coil in the future exams is expected to allow for a further increase in resolution at the expense of higher computational burden.

**Acknowledgments.** We acknowledge financial support of NIH R01NS065034 and R01NS066982.

**References.** [1] Nael K et al., Invest Radiol, 2006;41:391. [2] Tsao J, et al. MRM 2003;50:1031. [3] Johnson KM et al., MRM 2007;59:456. [4] Jung H et al., MRM, 2009;61:103. [5] Velikina JV et al. Proc. ISMRM 2010: 4876. [6] Bube KP, et al. Geophysics, 1997;62:1183. [7] Pruessmann KP et al., MRM 2001;41:638.